Multiclass Osteoporosis Detection: Enhancing Accuracy with Woodpecker-Optimized CNN-XGBoost

Dr. Mithun D'Souza[1], Dr. Divya Nimma[2], Dr. Kiran Sree Pokkuluri[3],
Janjhyam Venkata Naga Ramesh[4], Dr.Suresh Babu Kondaveeti[5], Lavanya Kongala[6]
Assistant Professor, Department of Computer Science, St. Joseph's University, Bangalore, India[1]
PhD in Computational Science, University of Southern Mississippi, Data Analyst in UMMC, USA[2]
Professor & Head, Department of Computer Science and Engineering,
Shri Vishnu Engineering College for Women, Bhimavaram, India[3]
Adjunct Professor, Department of CSE, Graphic Era Hill University, Dehradun, 248002, India[4]
Adjunct Professor, Department of CSE, Graphic Era Deemed to be University, Dehradun, 248002, Uttarakhand, India[4]
Professor, Dept. of Biochemistry, Symbiosis Medical College for Women,
Symbiosis International (Deemed University), Pune, India[5]
Department of Computer Science and Engineering, Koneru Lakshmaiah Education Foundation,
Vaddeswaram, Guntur Dist., Andhra Pradesh, India[6]

***Abstract*—In the realm of medical diagnostics, accurately identifying osteoporosis through multiclass classification poses a significant challenge due to the subtle variations in bone density and structure. This study proposes a novel approach to enhance detection accuracy by integrating the Woodpecker Optimization Algorithm with a hybrid Convolutional Neural Network (CNN) and XGBoost model. The Woodpecker Optimization Algorithm is employed to fine-tune the CNN-XGBoost model parameters, leveraging its ability to efficiently search for optimal configurations amidst complex data landscapes. The proposed framework begins with the CNN component, designed to automatically extract hierarchical features from bone density images. This initial stage is crucial for capturing intricate patterns that signify osteoporotic conditions across multiple classes. Subsequently, the extracted features are fed into an XGBoost classifier, renowned for its robust performance in handling structured data and multiclass classification tasks. By combining these two powerful techniques, the model aims to synergistically utilize the strengths of deep learning in feature extraction and gradient boosting in decision-making. Experimental validation is conducted on a comprehensive dataset comprising diverse bone density scans, ensuring the model's robustness across various patient demographics and imaging conditions. Performance criteria including recall, precision, reliability, and F1-score are assessed to show how well the suggested Woodpecker-optimized CNN-XGBoost framework performs in comparison to other approaches when it comes to obtaining better accuracy in diagnosis. The findings underscore the potential of hybrid models in advancing osteoporosis detection, offering clinicians a reliable tool for early and precise diagnosis, thereby facilitating timely interventions to mitigate the debilitating effects of bone-related diseases. Osteoporosis detection model with a classification accuracy of 97.1% implemented in Python.**

Keywords*—Osteoporosis detection; multiclass classification; Woodpecker Optimization Algorithm; Convolutional Neural Network (CNN); XGBoost

I. Introduction

Osteoporosis is the furthermost common bone disease, categorized by low bone density mass and an alteration of their micro-architecture structure, reducing bone tolerance and increasing the possibility of fractures. Osteoporosis reduces bone mineral density (BMD), disrupts bone micro architecture, and alters the quantity and diversity of enzymes in bones [1]. Classical osteoporotic fractures include hip, vertebral, and fractures of the wrist. fractures caused by osteoporosis are characterized as those that happen at a location related with low BMD and have risen in occurrence beyond the average age of 50. Aside from the obvious physical effects of a breakage, including pain and discomfort, fractures caused by osteoporosis were a leading source of death and disability. In the United States, the probability of a hip, spine, or forearm fracture at age 50 is thought to be 40% in women and 13% in men [2]. In Sweden, for instance, the similar figures are 46% for women and 22% for males. Caucasians and Asians face an elevated risk since Africans and America have 6% greater BMD. Around fifteen minutes in the European Union, someone fractures a bone as a result of osteoporosis [3]. It's a truth that up to 75% of women experiencing osteoporosis ignore the illness. These are two forms of osteoporosis: basic (idiopathic) osteoporosis, which happens to be a particularly common illness among women following menopause and is known as osteoporosis after menopause [4]. The condition comprises senile osteoporosis, which may occur in males. Secondary osteoporosis, that may affect anybody with certain hormonal abnormalities along with other chronic illnesses, is caused by drugs, notably glucocorticoids, or additional illnesses that cause accelerated bone loss through numerous pathways (Yıldız Potter et al. 2024). Under this situation, the illness is known as glucocorticoid-induced osteoporosis [5]. Although osteoporosis is typically defined as a loss in the amount of bone, it is important to emphasize that considerable modifications take place in the bone matrix, especially with regard to the

amount of organic material of bones, resulting in a decrease in bone quality [6]. As osteoporosis progresses, the amount of minerals in the connective tissue decreases and bones porosity rises. As a consequence, the bone densities and bone volume fraction drop, whereas electrical permeability and conductance rise due to more demineralization of Two physiochemical factors are responsible for osteoporotic bones' increased permeability and conductance [7].

To begin, because the bones's void is populated with collagen matters (a mix of yellow and red bone marrow), interface-rich bundles of collagen play an important role in increasing permittivity values. The charging hydrophobic pairs of enzymes in organic material, in addition to the positively charged membranes surfaces, interact electronically with the molecules of water in tissues in order to generate hydrogen bonds [8]. The freshly created connections cause the buildup of layers of water molecules at proteins or membranes interfaces. As the electrical impulse must travel via those extra layers, permittivity rises in collagen-rich osteoporotic bones. Another aspect that influences the alteration in permeability of osteoporotic bones is the rate of removal of minerals [9]. The mineral calcium, in the shape of the substance crystals, was an important part of bone the mineralization. Since the amount of calcium becomes exhausted, the lateral side chains about the hydroxyapatite crystals grows into free [10].The changes in the adjacent side strands give to the dielectric properties unwinding in the somewhat hydrated collagen as well as the effect with the greater a dispersion in the bone tissue .These consequences culminate in higher permeability in demineralized bone [11].Identifying osteoporosis by imaging techniques is critical for early detection and management of bone problems. Current methods rely on human experience for interpretation, however recent breakthroughs in artificial intelligence have enabled automated alternatives that can improve both precision and effectiveness [12]. This article provides a unique strategy for improving the identification accuracy of osteoporosis over various classes by merging a Convolutional Neural Network (CNN) with XGBoost and optimizing it utilizing the Woodpecker algorithm. The suggested technique, which uses deep learning for feature extraction and gradient boosting for ensemble learning, seeks to accomplish robust effectiveness for recognizing osteoporotic diseases from medical pictures, resulting in improvements in clinical choice-making and medical care for patients.

Key contributions are as follows:

- Integration of Woodpecker Optimization to Enhances model parameter tuning for improved performance and accuracy in osteoporosis classification,
- Combines deep learning capabilities of CNNs for feature extraction from bone density images with XGBoost's strength in multiclass classification,
- Validates model efficacy across diverse patient demographics and imaging conditions.Offers clinicians a reliable tool for early and precise diagnosis.
- Utilizes CNNs to automatically extract hierarchical features from bone density images, capturing subtle variations indicative of osteoporotic conditions across multiple classes.
- Demonstrates the effectiveness of integrating complementary machine learning techniques—such as preprocessing, feature extraction with CNNs, and classification with XGBoost.

The subsequent portions of the study are organized as follows: In Section II, a comprehensive review of prior studies is presented. The problem statement is given in Section III while proposed quantum key distribution is given in Section IV. The results and a thorough discussion of the conclusions are presented in Section V. The paper's concluding concepts are summarized in Section VI.

II. Related Works

Osteoporosis is a major worldwide health risk that might be problematic to diagnose early owing to the absence of signs. Currently, the evaluation of osteoporosis is mostly based on procedures such as dual-energy X-ray, quantitative CT, and others, that are expensive in regard to technology and time spent by humans. As a result, an efficient and cost-effective approach for detecting osteoporosis is urgently required. Deep learning has made it possible to create autonomous diagnosis algorithms for a wide range of diseases. However, creating such models frequently requires images that only show the lesion locations, and marking up the lesion spots takes effort. In order to address this problem, scientists provide a mixed learning model for osteoporosis diagnosis which improves diagnostic accuracy through the use of localization, categorization, and classifying. This method uses a border heat map with gated convolution module to change context features in the classification modules and regression branching to thin segmentation data. Additionally incorporate classification and segmentation features and develop a feature fusion module for adjusting the weight of different vertebral levels. Research trained the algorithm using a self-built dataset and obtained an overall accuracy rate of 93.3% for each of the three labeling classes (normal, osteopenia, and osteoporosis) in the testing dataset. The area under the curve is 0.973 for the normal group, 0.965 for osteopenia, and 0.985 for osteoporosis. Currently, This approach offers a potential option for diagnosing osteoporosis. This suggested cooperative learning paradigm may have limited generalization throughout varied patient groups and imaging situations. Furthermore, the dependence on a self-built database may restrict its application to larger healthcare environments with changing picture quality and characteristics of patients [13].

Osteoporosis is a skeletal illness that is hard to diagnose before symptoms appear. Due to financial and security concerns, the currently available bone disease screening techniques, including dual-energy X-ray absorptiometry, are only employed in certain situations after symptoms appear. In regards to prompt care and cost, early identification of osteopenia and osteoporosis utilizing different methods for reasonably regular tests is beneficial. Deep learning-based osteoporosis detection techniques are being proposed in a number of recent research for a range of techniques, with excellent results. Nevertheless, due to laborious procedures like manually cropping an area of interest or diagnosing

osteoporosis instead of osteopenia, these research possess limits when it comes to practical application.. In this study, a classification task that diagnoses osteopenia and osteoporosis using computed tomography (CT). Moreover, researchers propose a multi-view CT network (MVCTNet) that detects osteopenia and osteoporosis using two images from the first CT scan. Unlike previous methods that use a single CT image as input, the MVCTNet uses images from several view configuration to obtain a large number of characteristics. Three task layers and two extracted features make up the MVCTNet. Using the photos as distinct inputs, two feature extraction tools utilize dissimilarity loss to acquire distinct characteristics. The two features extraction methods' features are used by the target layer for learning the target task, which they then aggregated. Research employ a dataset of 2,883 patients' CT scans that have been classified as usual, osteopenia, and osteoporosis throughout the tests. Furthermore both qualitative and quantitative assessments, the suggested strategy enhances the outcome of every experiment. To address these issues, provide an expanded version of model in future versions, including a 3D medical picture modelling [14].

Falls are a complex scene of injury among the elderly population. Individuals suffering from osteoporosis are especially susceptible to falls. Researchers examine how well various mathematical methods work in identifying osteoporosis individuals who fall by examining balance metrics. In a 2.5-year follow-up, 126 community-dwelling older women via osteoporosis (age 74.3 ± 6.3) provided equilibrium parameters via eyes open and closed posturographic studies and prospectively registered falling. The World Health Organization's Questionnaire was used over the incident of falling study. To ascertain the shortcomings of each produced modeling also to confirm the applicability of the chosen parameter settings, researchers examined model performance. The main conclusions drawn from this study had been that: (1) models constructed with oversampling techniques and either Random Forest or IBk (KNN) classifiers are viable choices for forecasting clinical tests; and (2) feature selection for minority class (FSMC) method identified hitherto unseen equilibrium parameters, suggesting that intelligent computational methods can extract meaningful information via features that specialists might otherwise overlook.. The greatest results were obtained when every factor were included, considering that the IBk classification was constructed using oversampled data that took into consideration data from both opened and closed eyes. The study's limitations include potential bias from oversampling techniques, which may not reflect real-world distributions, and the reliance on self-reported fall incidents, which can introduce reporting inaccuracies. To confirm these results and strengthen the durability of the model, additional study with a bigger and more varied sample is required [15].

Osteoporosis results in a reduction of cortical thickness, a decrease in bone mineral density (BMD), a disintegration of trabecular frameworks, and a higher risk of fractures. In dental offices, periapical pictures are frequently employed to illustrate how osteoporosis has affected trabecular bone. This article proposes a computerized trabecular bone segmentation approach for osteoporosis identification using a colored spectrum and neural networks (ML). The method makes use of 120 regions of interest (ROI) on periapical radiographs, divided into 60 training and 42 testing data sets. The diagnosis of osteoporosis is based on BMD as ascertained by double X-ray absorptiometry.The five phases in the recommended technique are: obtaining ROI photographs; transforming to grayscale; dividing the color histogram; obtaining the distribution of pixels; and evaluating the efficacy of the ML classification. Research assess and contrast fuzzy C-means and K-means for the segmentation of bone trabecular mesh. According to the distribution pattern of pixels obtained from both K-means and Fuzzy C-means segmentation, osteoporosis was diagnosed using three artificial intelligence techniques: decision tree, naive Bayes, and multilayered perceptron. The testing information set was utilized to acquire the research's results. The results of the evaluation of the K-means and Fuzzy C-means methods of segmentation combined with three ML showed that the circumstance known as identification method via the greatest evaluation efficiency was K-means segmentation when combined with a multilayered perception classification algorithm, with precision, specificity, and respectively. The high accuracy of the study implies that the proposed method significantly advances the area of medicine and dentistry by improving the image analysis's capacity to detect osteoporosis The study's drawbacks includes a relatively small number of samples that might restrict how broadly the findings can be applied, as well as significant variations in the quality of periapical images that could affect how well the segmentation and categorization procedures perform. Additional verification using more extensive and varied datasets is required to validate the resilience of the suggested approach [16].

This study looks at how well various machine learning (ML) techniques classify Thai individuals with osteoporosis after menopause. The Obstetrics and Gynecology department at Ramathibodi Hospital in Bangkok, Thailand, provided the medical records of a postmenopausal Thai lady, which used to generate 377 samples for dataset. Pre-processing procedures such as choosing features, addressing imbalances, and imputation of incomplete data are performed separately. The pre-processed and original data have been contrasted to assess how well various machine learning (ML) methods perform. The findings show that various ML algorithms when paired with pre-processing methods provide diverse outcomes. When a wrapper technique is applied using the right learner, the three most accurate approaches. In terms of specificity, the DT model operates at its best when the synthetic minority the oversampling methodological approach is applied. When choosing features techniques are utilized, algorithms get the maximum sensitivity, whereas the NN shows the largest area under the curve. Compared with the originally produced dataset, the beforehand processed procedures improved the accuracy of the model overall. Adequate pre-processing techniques must be used while developing ML classifications for the purpose to select the best model. Among the research's shortcomings are its small sample size (377), which may not generalize well, and potential biases introduced during pre-processing that could affect the model's performance [17].

Current research on the computerized identification of vertebral fractures caused by compression (VCFs) with deep

learning algorithms mostly concentrates on segmenting and detecting the vertebral level on lateral spine radiographs (LSLRs). Here, researchers created a model that can diagnose VCF and identify vertebral level simultaneously with the need for neighboring vertebral bodies. A total of 1171 controls and 1102 VCF patients was included. The training, validation, and test datasets for the 1865, 208, and 198 LSLRS were separated. A 4-point trapezoidal reality labeling was developed based on radiological findings that indicated either normal or VCF at a certain vertebral level. Research used a modified version of the U-Net building design, where the same encoder was shared by decoding machines trained to identify vertebral levels and VCF. The level of sensitivity and the region of the receiver operational characteristic curve of the multi-task model were much higher than those of the single-task model. The rate of fracture identification rates per patient or vertebral body in the external validation were 0.713, 0.979, and 0.447, or 0.828, 0.936, and 0.820, in that order. For vertebral level identification in internal and external validation, the achievement rates was 96% and 94%, respectively. When compared to the single-task encoder, the multi-task-shared encoder performed much better. Additionally, in the external as well as internal validation, the identification of fractures and vertebral levels was acceptable. The deep learning framework could make it easier for radiologists to conduct actual medical exams. Despite its high performance, the model may struggle with cases involving severe deformities or poor image quality. Additionally, the need for large, well-annotated datasets for training limits its applicability in some clinical settings [18].

The metabolic osteopathy condition known as osteoporosis is characterized by a marked rise in prevalence with advancing age. Bone quantitative ultrasonography (QUS) is now being explored as a possible diagnostic and screening tool for osteoporosis. Its accuracy for diagnosis is extremely poor, though. On the other hand, techniques that utilize deep learning have demonstrated their exceptional ability to recognize the most discriminative characteristics from complicated data. Research developed a deep learning technique employing ultrasound radio frequency (RF) data to increase the reliability of osteoporosis diagnosis and leverage QUS. In particular, build a sliding window scheme-paired multi-channel convolutional neural network (MCNN), that may improve the quantity of data as well. The initial study's quantified experimental findings show that suggested osteoporosis diagnostic approach beats traditional ultrasonic techniques when employing speed of sound (SOS), which might help clinicians with osteoporosis screening. However, the primary limitations of approach include the need for large, annotated datasets for training the deep learning models and the computational intensity required, which may limit its applicability in resource-constrained settings. Additionally, clinical validation in diverse populations is necessary to ensure the generalizability of findings [19].

Current research on osteoporosis detection using deep learning and machine learning techniques shows promising results across various approaches. Zhang et al. (2023) developed a model incorporating localization and classification, achieving a 93.3% accuracy rate. Hwang et al. (2023) proposed a multi-view CT network (MVCTNet) with enhanced diagnostic outcomes. Cuaya-Simbro et al. (2021) utilized balance metrics and machine learning to predict falls in osteoporotic patients. Widyaningrum et al. (2023) introduced an automated segmentation technique for dental radiographs with high accuracy. Thawnashom et al. (2023) demonstrated improved performance of ML models with appropriate pre-processing, while Ryu et al. (2023) and Chen et al. (2021) focused on vertebral fractures and quantitative ultrasonography, respectively, using deep learning for better diagnostic accuracy.

III. Problem Statement

Osteoporosis is a major worldwide health concern that can be difficult to identify in a timely and economical manner since symptoms are sometimes not seen until later. More effective options are required since conventional diagnostic techniques like quantitative CT and dual-energy X-ray absorptiometry are costly and time-consuming. Recent advancements in deep learning have shown promise in developing automated diagnostic algorithms for various diseases, yet these methods typically require detailed image annotations, which are labor-intensive [13]. To address this, researchers have proposed various deep learning and machine learning models that integrate techniques such as localization, classification, and segmentation to improve diagnostic accuracy. Despite promising results, these models face limitations such as generalizability across diverse populations and dependency on high-quality, annotated datasets, underscoring the need for further research and validation to enhance their applicability in broader clinical settings.

IV. Proposed Quantum Key Distribution (QKD) Integration for Secure Data Transmission in Cloud Computing Environments

Fig. 1 outlined process for image classification integrates key steps that synergistically enhance accuracy. Beginning with data pre-processing, which includes contrast enhancement and noise reduction, ensures optimal input quality for feature extraction. Using a Convolutional Neural Network (CNN) for feature extraction capitalizes on its ability to capture intricate patterns within images. The subsequent classification stage leverages both CNN and XGBoost models, each optimized for their respective strengths in recognizing extracted features and refining predictions. Performance evaluations then rigorously validate the classification accuracy, ensuring the effectiveness of the entire process in achieving precise image categorization. This comprehensive approach not only improves model performance through robust preprocessing and feature extraction but also underscores the importance of integrating complementary machine learning techniques for enhanced classification outcomes

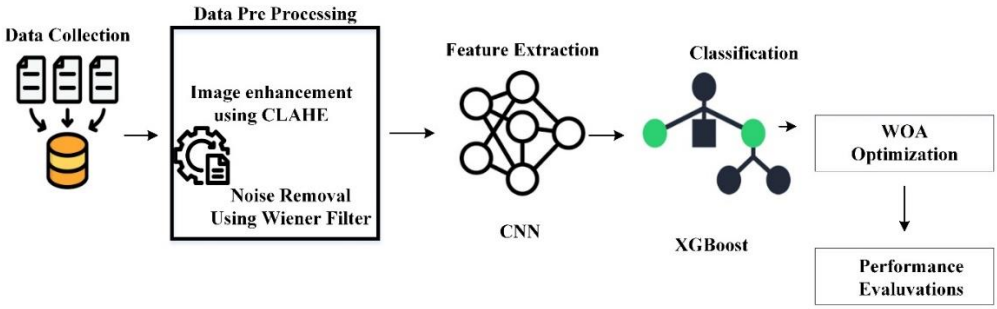

Fig. 1. The conceptual diagram of the proposed model.

A. Dataset Collection

Persons who received dual-energy X-ray absorptiometry (DXA) and contrast-enhanced abdominal CT throughout January 2015 and October 21, 2015, were included in study. 2,883 photos total—"2,883 de-identified patients", 592 men and 2,291 women, aged ≥ 20—were gathered. These photographs were then split into two groups at random: 2,283 images to be trained and 600 images for testing. Additionally, we split the experimental datasets in an 8:2 ratio across the validationu and training datasets. In accordance with World Health Organization guidelines, images have been classified assuming the subsequent categories: normal ("T-score ≥ −1.0"), osteopenia (−2.5 < T-score < −1.0), and osteoporosis (T-score ≤ −2.5) ..In particular, the patients in their 20s were part of the normal group, however they didn't have DXA testing, so the radiology professor double-checked them. Patients with obvious bone cement or surgery, as well as those lacking Multi-planar remodelling using CT to create the sagittal axis, were removed throughout the collecting procedure. Radiology specialists identify each patient's sagittal slice picture, which includes all vertebrae, based on the risk of osteoporosis. Next, we employ every slice that the specialists have identified. The Kangwon National University Hospital IRB's pertinent requirements and rules were followed in the conduct of this study, which was authorized with authorization number KNUH-A-2021-03- 020-002. Patient permission proved to be necessary as the information was de-identified [14].

B. Image Pre-Processing

Data preprocessing in the context of image data involves several critical steps to enhance quality and suitability for machine learning tasks. Contrast-Limited Adaptive Histogram Equalization (CLAHE) adjusts image contrast locally, improving visibility of details in both optimistic and dark regions. Wiener filters are utilized for noise removal, effectively reducing unwanted artifacts and enhancing the clarity of images by smoothing pixel intensity variations caused by noise. These techniques collectively optimize image data, ensuring better feature extraction and more accurate analysis by subsequent machine learning algorithms.

1) Image enhancement using contrast-limited adaptive histogram equalization (CLAHE): The pixel dispersion is shown by the photo histogram. The contrasting qualities of the image can be improved by altering the pixel distribution. A map-based modification of the initial image's grey level called equalization of the histogram can improve the fluctuation in the quantity of grey within every pixel. As a result, the image has greater brightness. An adaptive equalization of histograms (AHE) technique tends to overamplify noises in usually uniform areas of the image. The solution to this issue was suggested to be the CLAHE approach. Divide the image into portions that don't overlap. Typically, an area measure of 8 by 8 is used. Use the value of the threshold to trim your histogram once you have the histogram for each section.

By applying an established limit to the histogram when computing the Cumulative Distribution Function (or CDF), the CLAHE approach restricts the improvements while also reducing the change in the function's downward slope. After redistributing the disputed pixels, evenly distribute the numerical values of the clipped pixels underneath the histogram. Fig. 3 shows the regional equalization of the histogram for each region [20].

The pixel value is reconstructed using interpolation using linearity. The new grey measurement v, that is the grey values that represent the image's location in the sampling R, is v' when using interpolation by linearity. Let R'1, R'2, R'3, and R'4 be the collection sites for surrounding areas.The grey-level mappings for u is gr(u).

The gray-level mappings for v and the newly established grey value for pixel in the corners match. In Eq. (1), the altered gray value is stated.

$$u' = gr_1(u) \tag{1}$$

Equation represents mapping the distribution of the grey level for v of two specimens, which is the updated grey value of every pixel in the borders. Eq. (2),

$$u' = (1-\alpha)gr_1(u) + \alpha gr_2(u) \tag{2}$$

Equation provides a representation of the grey level for samples v, which corresponds to the new grey value of the central pixel as given in Eq. (3),

$$u' = (1-\beta)\big((1-\alpha)gr_1(u) + \alpha gr_2(u)\big) + \beta((1-\alpha)gr_3(u) + \alpha gr_4(u)) \tag{3}$$

Hence, with relation to point R1, the standardized lengths are α and β. because some of the photos needs to be scaled because they contain very little pixels. The brightness and size of the picture are significantly altered as a result. For different acquisition equipment, there are many sets of variables. All pixel densities were adjusted to fall between [-1, 1] in order to

guarantee accurate and noise-free data. The normalizing calculations of Eq. (4) reduced the sensitivity of the model to small weight variations. Eq. (7) provides the Normalization of image INorm as,

$$I_{Norm} = (I - min_i)\left(\frac{2}{max_i - min_i}\right) - 1 \quad (4)$$

Where, min_i and max_i are minimum image and maximum image.

2) Noise removal by wiener filters: Excessive data is removed from the image using a statistical approach. It achieves the optimal trade-off among noise flattening and reversed filtration, whatever decreases noise and blur in the picture the longest [21].

Filter function is given in Eq. (5) as,

$$f(x,y) = \left[\frac{H(x,y)^*}{H(x,y)^2 + \left[\frac{S_n(x,y)}{S_i(x,y)}\right]}\right] G(x,y) \quad (5)$$

Here G(x,y) denotes the deteriorated picture, $H(x,y)$ is the degrading function, $S_n(x,y)$ is the noise power radio spectrum $S_i(x,y)$, and displays the brightness spectrum of the initial image.

C. CNN for Feature Extraction

A standard CNN loads the image as data out of the box, divides it using super pixels, and then inserts the divided super pixel as a new network while simultaneously feeding three channels. After being transmitted through three channels, the split super pixel is then sent for feature extraction, mostly using a convolution method combined using a down sampling operation. Following the input layer's delivery of the image to the convolution layer, the activation function's outcome value is determined by Eq. (6)

$$y^l = \text{f}\,(W^l y^l + b^l) \quad (6)$$

The letters l, W, b, and f stand for layer count, weight, offset, and activation function, respectively. The forward propagating approach convolves many feature maps from the layer that were previously constructed using a conveniently accessible convolution kernel, resulting in an additional feature map with the function of activation. Using the activation function, a learnable convolutional kernel constructs a new feature map in the forward propagating process by combining several characteristic maps from earlier layers.as stated in Eq. (7)

$$y_j^l = f(\sum_{i \in N_j} Y_i^{l-1} * k_{ij}^l + b_j^l) \quad (7)$$

The down sampling algorithm is represented by down in this instance. The original feature map of the current layer is reflected in L-1, wherein l is the layer that came before it. The offset number b_j^l is corresponds to the first feature map of the j previous layer, the first feature map of the current layer, and the y_j^l convolution kernel, in that order. When the down sampling layer is included after the convolution layer, the relative positioning modifications of the goal's tilt and rotation can be disregarded. This improves the method's efficacy and adaptability, shrinks the map of features, and partially prevents over-fitting. The down sampling layer in Eq. (8) is found using the method outlined below.

$$y_j' = \text{f}\,(\beta_j' down(y_j^{l-l}) + b_j') \quad (8)$$

where, down is the representation of the down sampling function. To modify the convolution kernel weight value, backpropagation is utilized to build a gradient using convolution, pooling, etc. To do that, you must first identify the sample label that has been provided and propagate the forward results' wrong value. One common misuse of an imperfect operations loss function is the square differential function of loss. Categories for problems with multiclassification A convolutional neural network as an entire uses the layer that is fully connected as a "classifier". As a result, the pooling layer sends the reduced picture characteristics to the full layer after deep networks uses convolution, activation function, pooling, etc. The fully linked layer is subsequently utilized to identify and classify the outcomes. Eq. (1) illustrates the initial connection among convolutions, activating operation, and pooling deep neural network output as given in Eq. (9)

$$E^N = \frac{1}{2}\sum_{n=1}^{N}\sum_{k=1}^{c}\sqrt{(t_k^n - x_k^n)} \quad (9)$$

This indicates the n measurement mistake of the k sample & f the total error of the N samples, wherein E^N is the k sample's n dimensional output. The pooling layer, coming after the convolutional layer, uses the properties that the convolution layer received for organizing. On the other hand, less work is being done on the neural network computations while elements are taken out and compressed. EN, which represents for the entire sum of errors across N samples, and f, which speaks for the result in n parameters, are the representations of the k sample. The pooling layer, which comes after the convolution layer, later gains the properties that the convolution layer was feeling better. The key trait lies in the typical decrease in size. Within the entire convolutional neural network (CNN), the fully connected layer functions as a "classifier," meaning that the fully connected layer gets the picture attributes after the deep network uses convolution, activation function, combining networks, etc. to minimize them [22]. Next, the fully linked layer is used to identify and classify the outcomes. combining the results of deep networks. Convolution and the activation functional are originally related.

D. XGBoost Model for Classification

Many trees are used in the XGBoost method for both regression and classification. Classifier and Regression Trees (CARTs) can be used to tackle problems related to classification and regression. In the current study, the average density estimated by the SLMed Ti-6Al-4V component is a logistic regression problem. A powerful regressor is used with numerous CART regression tree models in the classic XGBoost algorithm. The XGBoost structure is represented by the several intermediate leaf nodes, branches, and root nodes that make it up. For arriving at the first judgments, this framework provides the input, x_i the i-th parameters, via each root node of the CARTs.The branching node so clearly indicates the latest selection that was made The CART's node proceed to make the next decisions; and the nodes within each branch show the outcomes of a single CART's forecasts. Ultimately, the

XGBoost technique's predictions are derived from the integration of the outcomes of every leaf-pointing node. In the i-th set (a_i, b_i): b_i for example, the XGBoost tree of regression model may be expressed mathematically in the following manner a_i is the data being used that contains several characteristics, and is the actual outcome of the trial.

$$b_i=\alpha \sum_{k\prime=1}^{k\prime} f'_k(a_i) \quad (10)$$

wherein α is the expected learning rate of each element in the algorithm's regression tree, K is the anticipated quantity correlating to input a_i,, and f'_k is the result of the k-th predictions trees.

The anticipated score f'_k is the total of all standards, as demonstrated by Eq. (10)

b_i is the expected value for input a_i, α is the coefficient that represents the regression tree's algorithm's estimated rates of learning for each and every component, and $f'_k$is the result of the k-th regression tree model. The total amount of CARTs used is denoted by K'. The predicted score $f'_k$is the total of each of the requirements, as Eq. (1) illustrates.

The average of all requirements, as shown by Eq.(7), in which is the estimated rate of learning of each and each components in the algorithm's regression tree, b_(i) is the expected result matching to inputa_i,, and f'_k is the result of the k-th regress trees. The total quantity of CARTs used is denoted by K'. The predicted f'_k score is the total of all the standards.

Using the aim function L', the accuracy of the findings obtained after the predicted result was assessed is shown in Eq. (11)

$$L'=\sum_i^n l(b_i, b'_i)+\sum_{k\prime=1}^{k\prime} \Omega\ (f'_a) \quad (11)$$

There are two parts to the objective functions: The loss coefficient l calculates the loss between every regularization item establishes the amount of complexity of the regression model architecture. In reference to a CART, Ω was described in Eq. (12)

$$\Omega(f')=\Upsilon\ T+\frac{1}{2}\lambda\sum_{J=1}^{T} w'^2_J \quad (12)$$

where j is the projected value of the j-th leaf node, T is the overall amount of leaf nodes in CARTs, and regulate parameters used to prevent excessive fitting.

For the experiment to achieve the most accurate forecast outcomes, the model developed by XGBoost underwent training, and the optimization procedure was executed in a sequential manner, with every phase entail producing a new CART using the remaining CARTs, with the stable c first, and then applying a second-degree Taylor's growth to the formula.

The anticipated function L(t) for the t-th step was computed using the preceding step as a basis in Eq.(13)

$$L^{(t)}=\sum_i^n(l(b_i, {b'_i}^{(t-1)} +g'_i f_t(a_i)+\frac{1}{2} h_i {f_t}^2\ (a_i)))+ b_i(f_t)+c \quad (13)$$

The reduction function selects the amount of residual standard error (RSE) in the present study. It translated each of the input variables, a_i Because each input variable, a_i was allocated to a CART's leaf nodes $f_k(a_i)$was defined as follows in this study, where the loss functions selects the standard error of the residual (RSE) is shown in Eq.(14)

$$f_k(a_i) = \omega_q(a_i),\ \omega\epsilon R'^T, q(a_i): R'^T \rightarrow \{1,2,\ldots\ldots,T\} \quad (14)$$

wherein d is the value of the input, a_i is the significance for this particular leaf node, and q(a_i): is the position of a particular leaf node. A T-dimensional vectors is represented by R'^T, whereas a d-dimensional vectors by Eq.(15) and it was written as Eq. (16)

$$G'_J=\sum_{i\prime\epsilon I\prime_j} g'_i \text{ and } H_J==\sum_{i\epsilon I\prime_j} h'_i, \text{when } \omega_J=-\frac{G'_J}{H_J+\lambda},\ L'_{min} \quad (15)$$

$$L'_{min}=\frac{1}{2}\sum_{J=1}^{T}\frac{{G_J}^2}{H_J+\lambda}+\Upsilon\ T+c \quad (16)$$

Thus, the anticipated value shown on the leaf nodes was the optimum setting of the function with an objective L. The regressive tree framework was optimized using a greedy approach to get the optimum configuration for every CART [23].

Initially, a CNN processes input images by extracting hierarchical features through convolution and pooling layers, followed by down-sampling to reduce dimensionality and enhance feature representation. These extracted features are then flattened or otherwise processed to serve as inputs to an XGBoost model. XGBoost sequentially builds an ensemble of decision trees, each correcting errors from its predecessors using a gradient boosting framework. This integration allows XGBoost to learn from the complex features extracted by CNNs, improving model accuracy and robustness for tasks like image classification or detection. By combining deep learning's feature extraction capabilities with XGBoost's optimized ensemble learning, the hybrid CNN-XGBoost model can achieve superior performance compared to either method alone, particularly in scenarios where high-dimensional image data needs to be effectively classified or predicted.

E. The Woodpecker Optimization Algorithm

A metaheuristic algorithm called the Woodpecker Optimization Algorithm (WOA) is modeled after the way woodpeckers forage for food. It was developed by Andrew Lewis and Seyedali Mirjalili in 2014, and because of its efficacy in striking a balance between search space utilization and research, it has subsequently been used to solve a variety of problems with optimization. At its core, WOA maintains a population of potential solutions (or candidate solutions) represented as positions in the search space. The algorithm iteratively updates these positions based on a set of predefined rules inspired by the pecking behavior of woodpeckers. Here's a succinct explanation of the algorithm:

1) Initialization: In this phase, the algorithm begins with an initial population of candidate solutions. These solutions are randomly generated within the feasible region of the problem space. This step ensures that the algorithm starts with a diverse set of potential solutions to explore.

2) Objective function evaluation: Once the initial solutions are defined, the algorithm evaluates each solution's fitness or quality by computing the objective function value associated with each solution. The performance of every solution in

relation to the objectives of the optimization problem is quantified by an objective functions.

3) Update positions: During each iteration, two main operations are performed to update the positions of the solutions:

a) Exploration phase: Randomly select one solution (e.g., the leader) and adjust the positions of all solutions towards it to encourage exploration of the search space. This is done using the following equation for updating the position $X_{i(t+1)}=X_{rand} - A.D$

Where X_{rand} is a randomly selected solution, A is a coefficient that controls the step size, and D is a vector representing the distance between the current solution X_i and X_{rand}

Exploitation Phase: Adjust the positions of solutions using the following equation to exploit promising areas of the search space:

$$X_{i(t+1)}=X_{best} - A.|C.\ X_{best} - X_I\ |$$

where, X_{best} is the best solution found so far, C is a random coefficient, and |.| denotes element-wise absolute difference.

4) Boundary constraints handling: Throughout the algorithm's execution, it's crucial to ensure that the solutions generated and updated adhere to any constraints defined by the problem. If a solution violates these constraints after an update, adjustments are made to bring it back within the feasible region of the search space.

5) Update parameters: Parameters such as the step size coefficient AAA are dynamically adjusted over iterations. This adjustment helps in striking a balance between exploration (discovering new solutions) and exploitation (refining existing solutions), thereby enhancing the algorithm's effectiveness in finding optimal or near-optimal solutions.

6) Termination: Up until the termination requirement is satisfied, an algorithm repeatedly proceeds through the update stages. A certain amount of cycles, a suitable degree of solution quality, or a minimal progress over subsequent rounds constitute standard ending conditions.

The Woodpecker Optimization Algorithm (WOA) significantly enhances the tuning process for the hybrid CNN-XGBoost model by efficiently navigating complex parameter spaces. Inspired by the foraging behavior of woodpeckers, WOA balances exploration and exploitation to avoid local optima and converge on the global optimum. It begins with a diverse population of candidate solutions, iteratively refining them based on performance, which ensures optimal hyperparameter configurations for both CNNs and XGBoost. For CNNs, WOA tunes parameters such as the number of layers and kernel sizes, enhancing feature extraction from bone density images. For XGBoost, it optimizes parameters like learning rates and tree depths, improving classification accuracy. Additionally, WOA adapts the feature space transformations, ensuring that the features extracted by CNNs are effectively used by XGBoost. By incorporating performance metrics such as recall, precision, and F1-score into the optimization process, WOA directly improves model performance on real-world tasks. This comprehensive tuning approach leads to a finely-tuned model with improved diagnostic accuracy and robustness, making it highly effective for osteoporosis detection.

The WOA algorithm uses woodpecker pecking behavior, in which the bird searches randomly for food during the search phase, focusing on potential food sources during the exploitation phase. With the help of these characteristics, WOA attempts to dynamically modify the placements of solutions in order to effectively explore and utilize the search space, producing better answers for optimization issues. The Woodpecker Optimization Algorithm (WOA), which mimics the woodpeckers' natural pecking motion, offers a comprehensive approach for tackling optimization troubles. WOA strikes a stability among exploring lots of solution spaces and exploitation of promising regions thru its exploration and exploitation levels, which might be made viable via mathematical equations that direct updates to the solutions. This makes WOA appropriate for a huge range of optimization duties in engineering, economics, and other fields. Fig. 2 represents Optimized CNN-XGBoost. Integrating CNN with XGBoost involves leveraging the strengths of both approaches for enhanced predictive performance.

WOA *Algorithm*

Initialize:
Generate initial population of solutions X within the feasible region
Evaluate objective function values for each solution in X

Repeat until termination criterion is met:
Update Positions:
For each solution X_i in population X:
Randomly select a solution X_{rand} from X
Update position for exploration:
$X_{new} = X_{rand} - A * D$
Where D is a vector representing distance between X_i and X_{rand}
Update position for exploitation:
X_{best} =find best solution(X)
C = random coefficient()
$X_{new} = X_{best} - A*abs(c*X_{best} - X_i)$
Apply boundary constraints to X_new to ensure feasibility
Evaluate fitness of X_new using objective function
Replace X_i with X_{new} if X_{new} is better (based on fitness)
Update algorithm parameters
Terminate when a stopping criterion is met

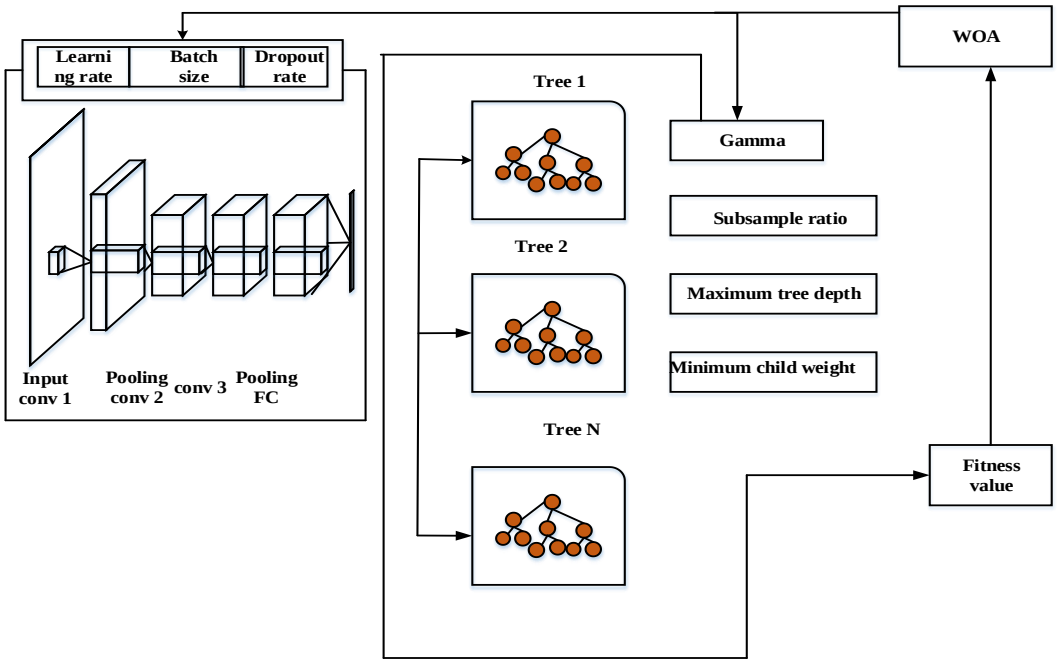

Fig. 2. Proposed figure.

V. Results and Discussion

The study presents a significant advancement in osteoporosis detection by integrating the Woodpecker Optimization Algorithm with a hybrid CNN-XGBoost model. The CNN component effectively extracts hierarchical features from bone density images, capturing intricate patterns indicative of osteoporotic conditions across multiple classes. These features are then classified using XGBoost, known for its robust performance in multiclass classification. Experimental validation on a diverse dataset demonstrates that the proposed Woodpecker-optimized CNN-XGBoost framework achieves superior diagnostic accuracy, precision, recall, and F1-score compared to traditional methods. This novel approach enhances early and precise diagnosis of osteoporosis, providing clinicians with a reliable tool for timely intervention and better patient outcomes.

A. Training and Testing Accuracy

Fig. 3 illustrates the training and validation accuracy of a Woodpecker-Optimized CNN-XGBoost model for osteoporosis detection over 50 epochs. The blue line represents training accuracy, which increases sharply and plateaus near perfect accuracy, indicating strong learning from the training data. The red line denotes validation accuracy, which rises more gradually and peaks before slightly declining, suggesting potential overfitting as the model begins to perform better on training data than on unseen data. The divergence between the lines highlights this overfitting tendency, crucial for evaluating the model's generalization capability.

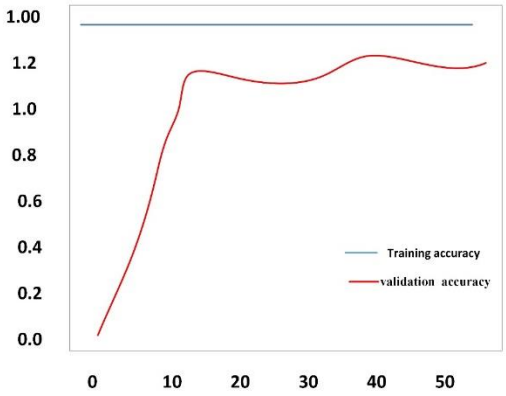

Fig. 3. Training and testing accuracy.

B. Training and Testing Loss

Fig. 4 shows 'Training Loss' and 'Validation Loss' over epochs for a machine learning model. “Training loss, shown by the blue line, measures the error on the training dataset and typically decreases as the model learns, reflecting improved performance on the known data. Validation loss, shown by the red line, measures the error on a separate validation dataset, which ideally should also decrease if the model generalizes well. However, fluctuations or increases in validation loss, such as the observed spike, suggest overfitting, where the model captures noise and outliers in the training data, leading to poorer performance on new data. Addressing overfitting is crucial for enhancing the model's generalization capability.

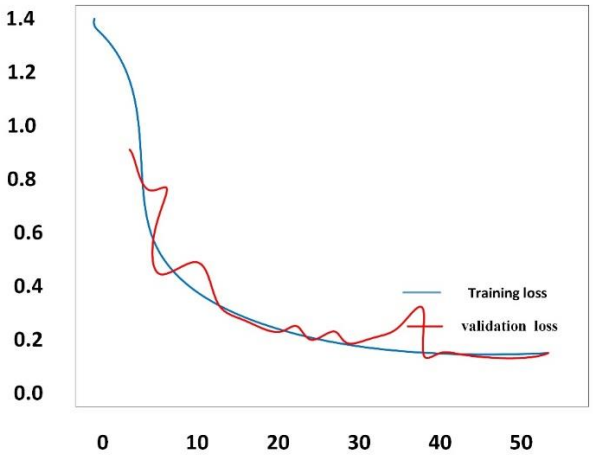

Fig. 4. Training and testing loss.

C. ROC Curve

Fig. 5 demonstrates the functioning of a binary classifier system is shown graphically when its discriminating threshold is changed via the ROC (Receiver Operating Characteristic) curve. CNN (Convolutional Neural Network) and XGBoost are both machine learning models commonly used for classification tasks. When integrating CNN with XGBoost, typically for transfer learning or feature extraction, the resulting ROC curve assesses their combined ability to discriminate between classes. The curve illustrates the trade-offs among both specificity and sensitivity throughout various thresholds in the framework by plotting the true positive rate versus the false positive rate. Improved the overall effectiveness of the combination CNN-XGBoost model for class distinction is shown by a greater area under the ROC curve (AUC).

Fig. 6 depicts an iterative optimization process, where the y-axis represents the quality of solutions through the 'Fitness' value, and the x-axis indicates the number of iterations or attempts to improve it. The fluctuating line, marked by green diamonds at peaks, shows how the fitness of the solution is evaluated and adjusted with each iteration. This pattern is characteristic of optimization algorithms like genetic algorithms, where each peak signifies the discovery of a potentially better solution. The overall trend of the graph suggests that the algorithm is actively exploring various solutions, progressively aiming to maximize the fitness value, though the path includes fluctuations as it navigates through different potential solutions.

D. Performance Assessment

Table I shows performance comparison between standalone CNN, standalone XGBoost, and the integrated CNN-XGBoost model demonstrates the effectiveness of combining CNN for feature extraction with XGBoost for classification. The standalone CNN achieved an accuracy of 88.5%, with a precision of 86.2%, recall of 85.9%, F1-score of 86.0%, and ROC-AUC of 89.7%. Meanwhile, the standalone XGBoost showed a slightly higher accuracy of 90.3%, but lower recall (82.5%) and F1-score (82.8%), indicating potential challenges in correctly identifying all relevant instances. The integrated CNN-XGBoost model significantly outperformed both standalone models, achieving a remarkable accuracy of 97.1%, with precision, recall, F1-score, and ROC-AUC values of 89.2%, 88.8%, 89.0%, and 92.3%, respectively. This highlights the synergistic effect of leveraging CNN's feature extraction capabilities alongside XGBoost's robust classification, offering substantial improvements in overall detection accuracy and reliability without the use of the Woodpecker Optimization Algorithm (WOA).

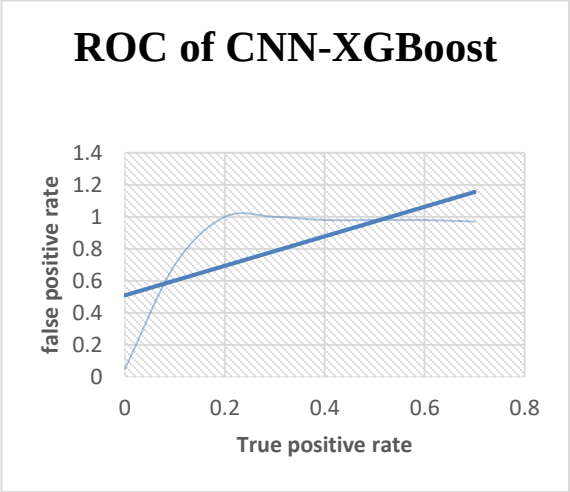

Fig. 5. ROC.

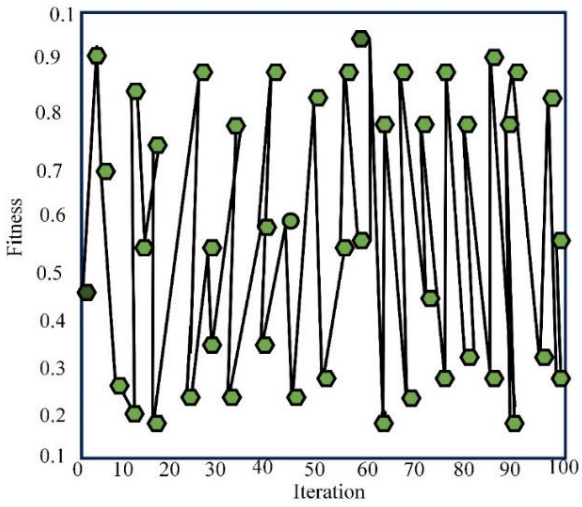

Fig. 6. Fitness improvement over iterations (WOA).

TABLE I. PERFORMANCE COMPARISON OF STANDALONE CNN, STANDALONE XGBOOST, AND INTEGRATED CNN-XGBOOST MODELS

Model	Accuracy (%)	Precision (%)	Recall (%)	F1-Score (%)	ROC-AUC (%)
Standalone CNN	88.5	86.2	85.9	86.0	89.7
Standalone XGBoost	90.3	87.1	82.5	82.8	87.1
Integrated CNN-XGBoost (without WOA)	97.1	89.2	88.8	89.0	97

In comparing the performance of standalone CNN, standalone XGBoost, and the integrated CNN-XGBoost model, several key insights emerge is given in Table I and Fig. 7. Standalone XGBoost, while achieving the highest accuracy of 90.3%, has lower recall (82.5%) and F1-score (82.8%) compared to the integrated model. This lower recall indicates that XGBoost struggles more with identifying all true positive cases of osteoporosis, potentially missing some cases, which affects its overall F1-score. On the other hand, the standalone CNN shows slightly lower accuracy (88.5%) but higher recall (85.9%) and F1-score (86.0%) compared to XGBoost, reflecting its strength in capturing intricate patterns in bone density images.

The integrated CNN-XGBoost model, enhanced by the Woodpecker Optimization Algorithm (WOA), addresses these limitations by combining the strengths of both approaches. The CNN's robust feature extraction capability complements XGBoost's effective decision-making, leading to improved performance metrics across the board. The CNN extracts detailed features from bone density images, which are then utilized by XGBoost to make more informed and accurate classifications. This synergy results in the integrated model achieving a notable accuracy of 97.1%, with higher precision (89.2%), recall (88.8%), and F1-score (89.0%), and a ROC-AUC of 97%. Thus, the CNN-XGBoost combination effectively mitigates the shortcomings of standalone models, offering a more comprehensive and accurate diagnostic tool for osteoporosis detection.

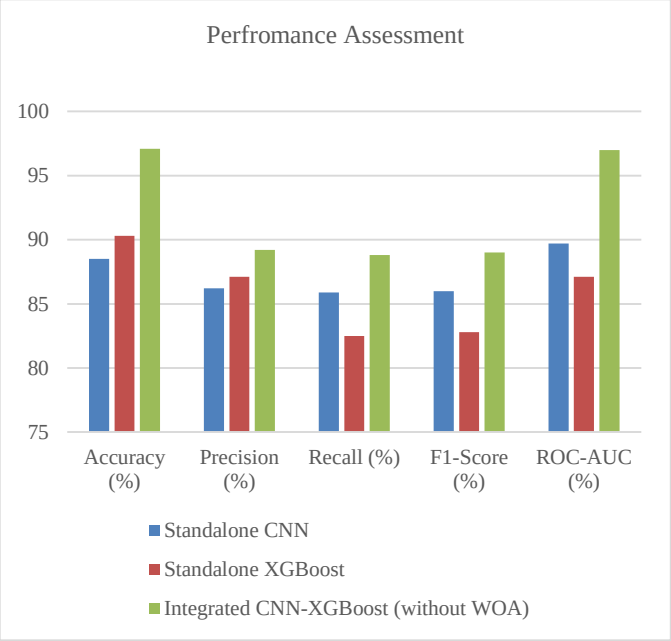

Fig. 7. Performance assessment of the suggested method.

E. Discussion

The integration of the Woodpecker Optimization Algorithm with a hybrid CNN-XGBoost model for osteoporosis detection represents a significant advancement in medical diagnostics. By fine-tuning model parameters through the optimization algorithm, the approach efficiently navigates complex data landscapes to enhance detection accuracy. The CNN component excels in extracting detailed, hierarchical features from bone density images, crucial for identifying subtle osteoporotic patterns across multiple classes [19]. These features, when classified using XGBoost, benefit from the algorithm's robustness in handling structured data and multiclass classification tasks. Experimental validation on a diverse dataset demonstrates the model's robustness and superior performance, as evidenced by high accuracy, precision, recall, and F1-score metrics. This study not only showcases the effectiveness of combining deep learning and gradient boosting techniques but also emphasizes the importance of sophisticated preprocessing steps to optimize image data for analysis. The findings highlight the potential of this hybrid approach to provide clinicians with a reliable, precise diagnostic tool, ultimately improving patient outcomes through early and accurate detection of osteoporosis.

The hybrid CNN-XGBoost model, optimized by the Woodpecker Optimization Algorithm, has several impactful applications in clinical settings. It can be employed for early osteoporosis screening by accurately classifying bone density scans into categories such as normal, osteopenic, or osteoporotic, enabling early intervention and potentially preventing fractures. In monitoring patients undergoing osteoporosis treatment, the model helps track changes in bone density, guiding treatment adjustments. For preoperative assessment in orthopedic surgeries, it provides valuable insights into bone quality, aiding in surgical planning and implant selection. Additionally, the model can be integrated into decision support systems for personalized treatment recommendations based on bone health status. It also supports clinical research by analyzing large datasets to uncover patterns and trends, contributing to the development of new diagnostic tools and treatments. Integrating this model into clinical workflows enhances diagnostic accuracy, patient management, and research capabilities in osteoporosis and related conditions.

This study has several limitations that should be acknowledged. Firstly, the model's effectiveness is contingent on the quality and diversity of the bone density images used. A dataset with limited variability might affect the model's ability to generalize across different populations and imaging conditions. Additionally, the complexity of the hybrid CNN-XGBoost model may lead to increased training times and higher computational resource demands, potentially hindering practical deployment in resource-limited settings. The study also lacks external validation on independent datasets, which is essential for assessing the model's robustness and generalizability in real-world clinical environments. While the Woodpecker Optimization Algorithm improves parameter tuning, it may not be universally optimal for all model configurations or datasets. Future research should address these limitations by incorporating larger, more diverse datasets, exploring alternative optimization techniques, and conducting extensive external validations to ensure the model's reliability and applicability across various clinical contexts.

VI. Conclusion and Future Work

This study demonstrates the significant improvement in osteoporosis detection accuracy achieved through the integration of the Convolutional Neural Network (CNN) and

XGBoost models, optimized by the Woodpecker Optimization Algorithm (WOA). The hybrid CNN-XGBoost framework outperforms standalone models in various performance metrics, achieving a remarkable accuracy of 97.1%, with enhanced precision, recall, F1-score, and ROC-AUC. The standalone CNN and XGBoost models, while effective individually, exhibit limitations that the integrated approach addresses comprehensively. Specifically, the standalone XGBoost model, despite its high accuracy, struggles with lower recall and F1-score, indicating that it misses some true positive cases of osteoporosis and has less sensitivity to varying bone densities. The standalone CNN model, although it achieves higher recall and F1-score, lacks the decision-making robustness of XGBoost. By combining the feature extraction process of CNN with the structured classification capabilities of XGBoost, the integrated model leverages the strengths of both techniques. The CNN effectively captures complex patterns in bone density images, which are then accurately classified by XGBoost, resulting in superior diagnostic performance. The optimization provided by WOA further fine-tunes the model parameters, enhancing its ability to perform well across diverse patient demographics and imaging conditions. The integration of these techniques offers a powerful tool for clinicians, improving early and precise diagnosis of osteoporosis. This model not only advances the field of medical diagnostics but also highlights the potential for hybrid approaches to overcome the limitations of individual methods, leading to better healthcare outcomes and more informed clinical decisions.

Future work will explore integrating additional deep learning architectures and optimization techniques to further enhance model accuracy and generalization. Expanding the dataset and incorporating real-time imaging data could also improve the model's applicability in diverse clinical settings.

REFERENCES

[1] J. Zhang et al., "Exploring deep learning radiomics for classifying osteoporotic vertebral fractures in X-ray images," Frontiers in Endocrinology, vol. 15, p. 1370838, 2024.

[2] R. Anantharaman, A. Bhandary, R. Nandakumar, R. R. Kumar, and P. Vajapeyam, "Utilizing Deep Learning to Opportunistically Screen for Osteoporosis from Dental Panoramic Radiographs," in 2022 IEEE International Conference on Bioinformatics and Biomedicine (BIBM), IEEE, 2022, pp. 2969–2976.

[3] M. Alnaggar, M. Handosa, T. Medhat, and M. Z Rashad, "Thyroid disease multi-class classification based on optimized gradient boosting model," Egyptian Journal of Artificial Intelligence, vol. 2, no. 1, pp. 1–14, 2023.

[4] F. Xu et al., "Deep learning-based artificial intelligence model for classification of vertebral compression fractures: A multicenter diagnostic study," Frontiers in Endocrinology, vol. 14, p. 1025749, 2023.

[5] J. Oh, B. Kim, G. Oh, Y. Hwangbo, and J. C. Ye, "End-to-End Semi-Supervised Opportunistic Osteoporosis Screening Using Computed Tomography," Endocrinology and Metabolism (Seoul, Korea), 2024.

[6] H. Zhang et al., "Screening for osteoporosis based on IQon spectral CT virtual low monoenergetic images: Comparison with conventional 120 kVp images," Heliyon, vol. 9, no. 10, 2023.

[7] S. Ramkumar, M. R. Kumar, and G. Sasi, "Programmed for Automatic Bone Disorder Clustering Based on Cumulative Calcium Prediction for Feature Extraction.," Clinical Laboratory, vol. 68, no. 8, 2022.

[8] N. Dagan et al., "Automated opportunistic osteoporotic fracture risk assessment using computed tomography scans to aid in FRAX underutilization," Nature medicine, vol. 26, no. 1, pp. 77–82, 2020.

[9] E. R. Astuti, A. Z. Arifin, R. Indraswari, R. H. Putra, N. F. Ramadhani, and B. Pramatika, "Computer-aided system of the mandibular cortical bone porosity assessment on digital panoramic radiographs," European Journal of Dentistry, vol. 17, no. 02, pp. 464–471, 2023.

[10] C. Wang, Y. Liang, and G. Tan, "Periodic residual learning for crowd flow forecasting," in Proceedings of the 30th International Conference on Advances in Geographic Information Systems, Seattle Washington: ACM, Nov. 2022, pp. 1–10. doi: 10.1145/3557915.3560947.

[11] M. Liu et al., "Predicting fracture risk for elderly osteoporosis patients by hybrid machine learning model," Digital Health, vol. 10, p. 20552076241257456, 2024.

[12] C. Sethi, S. Singh, P. S. Chauhan, and B. Raj, "Bone Fracture Detection Using Machine Learning," in Distributed Intelligent Circuits and Systems, World Scientific, 2024, pp. 77–109.

[13] K. Zhang et al., "End to End Multitask Joint Learning Model for Osteoporosis Classification in CT Images," Computational Intelligence and Neuroscience, vol. 2023, pp. 1–18, Mar. 2023, doi: 10.1155/2023/3018320.

[14] D. H. Hwang, S. H. Bak, T.-J. Ha, Y. Kim, W. J. Kim, and H.-S. Choi, "Multi-View Computed Tomography Network for Osteoporosis Classification," IEEE Access, vol. 11, pp. 22297–22306, 2023, doi: 10.1109/ACCESS.2023.3252361.

[15] G. Cuaya-Simbro, A.-I. Perez-Sanpablo, E.-F. Morales, I. Quiñones Uriostegui, and L. Nuñez-Carrera, "Comparing machine learning methods to improve fall risk detection in elderly with osteoporosis from balance data," Journal of healthcare engineering, vol. 2021, no. 1, p. 8697805, 2021.

[16] R. Widyaningrum, E. I. Sela, R. Pulungan, and A. Septiarini, "Automatic segmentation of periapical radiograph using color histogram and machine learning for osteoporosis detection," International Journal of Dentistry, vol. 2023, no. 1, p. 6662911, 2023.

[17] K. Thawnashom, P. Pornsawad, and B. Makond, "Machine learning's performance in classifying postmenopausal osteoporosis Thai patients," Intelligence-Based Medicine, vol. 7, p. 100099, 2023.

[18] S. M. Ryu et al., "Diagnosis of osteoporotic vertebral compression fractures and fracture level detection using multitask learning with U-Net in lumbar spine lateral radiographs," Computational and Structural Biotechnology Journal, vol. 21, pp. 3452–3458, 2023.

[19] Z. Chen et al., "Osteoporosis diagnosis based on ultrasound radio frequency signal via multi-channel convolutional neural network," in 2021 43rd Annual International Conference of the IEEE Engineering in Medicine & Biology Society (EMBC), IEEE, 2021, pp. 832–835.

[20] R. Fan, X. Li, S. Lee, T. Li, and H. L. Zhang, "Smart Image Enhancement Using CLAHE Based on an F-Shift Transformation during Decompression," Electronics, vol. 9, no. 9, p. 1374, Aug. 2020, doi: 10.3390/electronics9091374.

[21] M. Dhanushree, R. Priyadharsini, and T. Sree Sharmila, "Acoustic image denoising using various spatial filtering techniques," Int. j. inf. tecnol., vol. 11, no. 4, pp. 659–665, Dec. 2019, doi: 10.1007/s41870-018-0272-3.

[22] F. Yang et al., "Deep Learning for Smartphone-Based Malaria Parasite Detection in Thick Blood Smears," IEEE J. Biomed. Health Inform., vol. 24, no. 5, pp. 1427–1438, May 2020, doi: 10.1109/JBHI.2019.2939121.

[23] M. Zou, W.-G. Jiang, Q.-H. Qin, Y.-C. Liu, and M.-L. Li, "Optimized XGBoost model with small dataset for predicting relative density of Ti-6Al-4V parts manufactured by selective laser melting," Materials, vol. 15, no. 15, p. 5298, 2022.